

# Houttuynia cordata Thunb Promotes Activation of HIF-1A–FOXO3 and MEF2A Pathways to Induce Apoptosis in Human HepG2 Hepatocellular Carcinoma Cells

Integrative Cancer Therapies  
2017, Vol. 16(3) 360–372  
© The Author(s) 2016  
Reprints and permissions:  
sagepub.com/journalsPermissions.nav  
DOI: 10.1177/1534735416670987  
journals.sagepub.com/home/ict  


Jung Min Kim, PhD<sup>1\*</sup>, In-Hu Hwang, MD<sup>2\*</sup>, Ik-Soon Jang, PhD<sup>3\*</sup>, Min Kim, MS<sup>3</sup>, In Seok Bang, PhD<sup>4</sup>, Soo Jung Park, MD<sup>5</sup>, Yun-Jo Chung, PhD<sup>6</sup>, Jong-Cheon Joo, MD<sup>7</sup>, and Min-Goo Lee, MD, PhD<sup>2</sup>

## Abstract

*Houttuynia cordata* Thunb (*H cordata*), a medicinal plant, has anticancer activity, as it inhibits cell growth and induces cell apoptosis in cancer. However, the potential anti-cancer activity and mechanism of *H cordata* for human liver cancer cells is not well understood. Recently, we identified hypoxia-inducible factor (HIF)-1A, Forkhead box (FOX)O3, and MEF2A as proapoptotic factors induced by *H cordata*, suggesting that HIF-1A, FOXO3, and MEF2A contribute to the apoptosis of HepG2 hepatocellular carcinoma cells. FOXO3 transcription factors regulate target genes involved in apoptosis. *H cordata* significantly increased the mRNA and protein expression of HIF-1A and FOXO3 and stimulated MEF2A expression in addition to increased apoptosis in HepG2 cells within 24 hours. Therefore, we determined the potential role of FOXO3 on apoptosis and on *H cordata*-induced MEF2A in HepG2 cells. HIF-1A silencing by siRNA attenuated MEF2A and *H cordata*-mediated FOXO3 upregulation in HepG2 cells. Furthermore, *H cordata*-mediated MEF2A expression enhanced caspase-3 and caspase-7, which were abolished on silencing FOXO3 with siRNA. In addition, *H cordata* inhibited growth of human hepatocellular carcinoma xenografts in nude mice. Taken together, our results demonstrate that *H cordata* enhances HIF-1A/FOXO3 signaling, leading to MEF2A upregulation in HepG2 cells, and in parallel, it disturbs the expression of Bcl-2 family proteins (Bax, Bcl-2, and Bcl-xL), which results in apoptosis. Taken together, these findings demonstrate that *H cordata* promotes the activation of HIF-1A–FOXO3 and MEF2A pathways to induce apoptosis in human HepG2 hepatocellular carcinoma cells and is, therefore, a promising candidate for antitumor drug development.

## Keywords

*Houttuynia cordata*, HIF-1A, FOXO3, MEF2A, HepG2, apoptosis

Submitted Date: 19 January 2016; Revised Date: 21 August 2016; Acceptance Date: 27 August 2016

## Introduction

*Houttuynia cordata* Thunb (*H cordata*) is a medicinal plant that is considered to have anti-inflammatory and antiviral effects,<sup>1</sup> antiobesity effects,<sup>2</sup> and anticancer activity because it inhibits cell growth and induces apoptosis in human colorectal cancer,<sup>3,4</sup> leukemic cancer,<sup>5</sup> and lung cancer cells.<sup>6</sup> However, the potential anticancer activity and mechanisms of *H cordata* in human liver cancer cells have not yet been investigated. Therefore, we aimed to determine whether *H cordata* has anti-liver cancer activity and whether such effects are associated with induction of apoptosis in the human liver cancer line HepG2.

The ability to induce apoptosis is an important marker for cytotoxic antitumor agents. Some natural compounds have been shown to modulate apoptosis pathways that are

<sup>1</sup>Daejeon Oriental Hospital of Daejeon University, Daejeon, Republic of Korea

<sup>2</sup>Korea University College of Medicine, Seoul, Republic of Korea

<sup>3</sup>Korea Basic Science Institute, Daejeon, Republic of Korea

<sup>4</sup>Hoseo University, Asan, Republic of Korea

<sup>5</sup>Woosuk University, Jeonju, Jeonbuk, Republic of Korea.

<sup>6</sup>Chonbuk National University, Jeonju, Republic of Korea

<sup>7</sup>Wonkwang University, Iksan, Republic of Korea

\* Jung Min Kim, In-Hu Hwang, and Ik-Soon Jang contributed equally to this work. This article has been edited by Editage, a professional editing services company.

### Corresponding Authors:

Jong-Cheon Joo, Department of Sasang Constitutional Medicine, Wonkwang University, Iksan, Jeonbuk, 54538, Republic of Korea.  
Email: jcjoo@wku.ac.kr

Min-Goo Lee, Department of Physiology, Korea University College of Medicine, Seoul, Republic of Korea.  
Email: mingoolee@korea.ac.kr



Creative Commons Non Commercial CC-BY-NC: This article is distributed under the terms of the Creative Commons

Attribution-NonCommercial 3.0 License (<http://www.creativecommons.org/licenses/by-nc/3.0/>) which permits non-commercial use, reproduction and distribution of the work without further permission provided the original work is attributed as specified on the SAGE and Open Access pages (<https://us.sagepub.com/en-us/nam/open-access-at-sage>).

frequently blocked in human cancers and, thus, provide novel opportunities for cancer drug development.<sup>7</sup> Hypoxia-inducible factor 1 $\alpha$  gene (*HIF-1A*) is a subunit of the heterodimeric transcription factor hypoxia-inducible factor 1 (HIF-1).<sup>8,9</sup> HIF-1A functions as a tumor promoter in cancer-associated fibroblasts and as a tumor suppressor in breast cancer cells.<sup>10</sup> HIF-1A increases the risk of castrate resistance and metastases in prostate cancer<sup>11</sup> and metastases in patients on androgen deprivation therapy for prostate cancer.<sup>12</sup> Conversely, HIF-1 significantly promotes apoptosis via several proapoptotic target genes, RTP801, and the Bcl-2 family of proapoptotic factors.<sup>13,14</sup> Forkhead box proteins are a family of transcription factors, including FOXO1 (FKHR), FOXO3 (FKHRL1), FOXO4 (AFX), and FOXO6, which have been implicated in cell growth, proliferation, differentiation, apoptosis, and longevity.<sup>15,16</sup> Previous studies have demonstrated that Akt/protein kinase B phosphorylates FOXO transcription factors, which attenuates the nuclear translocation of FOXOs and their binding with 14-3-3 protein, resulting in proteasomal degradation.<sup>17,18</sup> Furthermore, FOXO3, a Forkhead box class O (FOXO) transcription factor, is known to be a key tumor suppressor in breast cancer.<sup>15</sup> Conversely, FOXO3 and FOXM1 are known to be key players in cancer initiation, progression, and drug resistance.<sup>19</sup> Therefore, we designed experiments to dissect the mechanisms that regulate FOXO3 and apoptosis and to elucidate the potential role of FOXO3 in *H cordata*-mediated apoptosis in HepG2 cells.

In the present study, we investigated the apoptotic pathway induced by *H cordata* extract in HepG2 cells. The data herein clearly showed that *H cordata* triggers the activation of HIF-1A-FOXO3 and MEF2A pathways and the caspase-3- and caspase-7-mediated pathways to cause cancer cell death.

## Methods

### Plant Material, Extraction, and Fractionation

The dried whole plant of *H cordata* Thunb was procured from Hanwoori Herbs Company (Seoul, Korea). A voucher specimen (BP1234283) was deposited at the Korean Collection for Type Cultures and Biological Resource Center in the Korea Research Institute of Bioscience and Biotechnology (Jeongeup, Jeollabuk, Korea). Dried whole plants of *H cordata* (100 g) were extracted with 1 L of methanol (MeOH) in a shaking incubator at room temperature for 24 hours. The residue was re-extracted twice under the same conditions. The resulting extract was filtered through a 0.45- $\mu$ m filter, evaporated to dryness using a vacuum rotary evaporator (Rotavapor, Switzerland) at 80°C, and weighed (6.002 g W/W, dry base) to determine the yield of soluble constituents. The crude dried MeOH extract was then suspended in water and partitioned by ethyl acetate (EtOAc; 0.872 g) fractionation.

### LC-MS Analysis of *H cordata* Extract

Agilent 6410B Triple Quadrupole liquid chromatography mass spectroscopy (LC MS; Agilent Technologies, Wilmington, DE) equipped with an Electrospray ionization (ESI) source was used for the analysis. Sample weighing 100 mg was mixed with 1 mL of MeOH and centrifuged. Aliquots of 5  $\mu$ L of the processed samples were injected into the HPLC system (1200 Series LC, Agilent Technologies) fitted with Phenomenex Synergi Hydro-RP 4  $\mu$ m, 80 Å, 150  $\times$  2 mm<sup>2</sup> column, maintained at 30°C. ESI was operating at +3000 V and a source temperature of 380°C. Capillary voltage, cone voltage, and source offset were set at 3 kV, 30 kV, and 30 V, respectively. The gas flow of desolvation and the cone was set at 650 L/h and 150 L/h, with a nebulizer pressure of 15 bar. A mobile phase composed of 0.1% formic acid in distilled water (buffer A) and 0.1% formic acid in acetonitrile (buffer B) was used to separate the analysis specimens and pumped into the ESI chamber at a flow rate of 0.5 mL/min for 20 minutes. Fragmentor voltage and collision voltage were set at 90 and 20 V, respectively. Detection of the sample was carried out in the multiple-reaction monitoring mode (MRM) by monitoring the transition pairs of m/z 252.1  $\rightarrow$  136.1.

### Cell Culture

Human liver HepG2 hepatocellular cells were purchased from the American Type Culture Collection (Rockville, MD, USA). Cells were grown in DMEM supplemented with 10% (v/v) FBS (Gibco/Invitrogen, Grand Island, NY) and 1% (w/v) penicillin-streptomycin (Gibco/Invitrogen) in a 37°C incubator with 5% (v/v) CO<sub>2</sub> in a humidified atmosphere. Cells were grown to confluence, trypsinized, and then sub-cultured.

### Fluorescence-Assisted Cytometric Spectroscopy

To detect apoptosis, propidium iodide (PI)-annexin-V staining was performed using an Annexin-V-FLUOS Staining Kit according to the manufacturer's instructions. Briefly, HepG2 cells were treated with 1 and 10  $\mu$ g/mL of *H cordata* EtOAc fraction for 24 hours, harvested, and washed twice with phosphate buffered saline (PBS). The cell suspension was centrifuged at 2000 rpm (1200g) for 2 minutes and was then incubated with 0.2 mg/mL Annexin-V-FLUOS and 1.4 mg/mL PI for 15 minutes at room temperature. Staining was measured using an Image Cytometer (NUCLEOCOUNTER NC-3000, ChemoMetec, Copenhagen, Denmark) at an excitation of 488 nm with a 530/30 nm band pass filter to detect Annexin-V and a 670 nm high-pass filter to detect PI.

### Acquired Nuclear Fraction

HepG2 cells were prepared by incubation with a medium for 2 days. The cells were scraped, and 2 mL was added per

dish of homogenization buffer A (25 mM Tris [pH 7.5], 2 mM EDTA, 0.5 mM EGTA, 1 mM DTT, protease inhibitor cocktail, 1 mM PMSF, and 0.02% Triton X-100), and it was homogenized 15 times using a 15-mL Dounce homogenizer with pestle A, and centrifuged at 100 000g for 30 minutes. The supernatant cytosolic fraction was transferred into a new tube, and 500  $\mu$ L of homogenization buffer B (homogenization buffer A containing 1% Triton X-100) was added to the pellet. The pellet was resuspended by sonication, incubated for 30 minutes at 4°C by rocking, and centrifuged at 100 000g for 30 minutes. The supernatant nuclear fraction was transferred into a fresh tube. The protein contents of the cytosolic and nuclear fractions were determined using a bicinchoninic acid (BCA) assay kit (Thermo Scientific, Rockford, IL) and analyzed by western blotting against anti- $\beta$ -catenin antibodies.

### Western Blot Analysis

HepG2 cells were treated with *H cordata* EtOAc fraction (1 and 10  $\mu$ g/mL) for 24 hours, harvested, and washed twice with PBS. The cells were lysed using a lysis buffer from iNtRON (Seoul, Korea), and protein concentration was determined using a BCA protein assay kit (Pierce Chemical, Rockford, IL, USA), according to the manufacturer's protocol. Then, 30  $\mu$ g of denatured proteins were separated using 10% polyacrylamide gel electrophoresis and transferred onto nitrocellulose membranes. The membranes were blocked for 1 hour with 5% (w/v) skimmed milk in 0.1% Tween-20 and Tris-buffered saline (TTBS). They were then incubated with diluted (1:1000) primary antibodies against Bax, Bcl-2, Bid, tBid, caspase-3, caspase-7, caspase-9, p-AKT, and PARP (all from Cell Signaling Technologies, Beverly, MA) and AKT, FOXO3, HIF-1A, MEF2A, and p-FOXO3 (all from Abcam, Cambridge, MA). The membranes were washed thrice with TTBS for 5 minutes, followed by incubation with diluted horseradish peroxidase-conjugated goat antimouse or rabbit antigoat IgG (1:2000) in TBS containing 5% (w/v) skimmed milk at room temperature for 1 hour. The membranes were then rinsed thrice with TTBS for 5 minutes, and an enhanced chemiluminescence system (Thermo Scientific, San Jose, CA) was used to visualize the bands on a ChemiDoc MP system (Bio-Rad, Hercules, CA).

### RNA Extraction

Total RNA was extracted using TRIzol reagent (Life Technologies, Carlsbad, CA) according to the manufacturer's protocol. RNase-free DNase I (Promega, Madison, WI) was used to reduce the DNA contamination. Total RNA concentration and purity were determined by measuring the absorbance ratio at 260:280 nm in a spectrophotometer (RNA samples with ratios greater than 1.8 were used for the

analyses). The integrity of the RNA samples was also ascertained by analyzing 28S and 18S ribosomal RNA using a Bioanalyzer 2100 system (Agilent Technologies, Santa Clara, CA).

### Gene Expression Profiles

For microarray analysis, HepG2 cells ( $1 \times 10^6$  cells) were seeded into 100-mm-diameter cell culture dishes. After 24 hours, the cells were treated with 1 or 10  $\mu$ g/mL *H cordata* extract for 6 hours. For control and test RNAs, synthesis of target cRNAs and hybridization were performed using the Low RNA Input Linear Amplification Kit PLUS (Agilent Technology) according to the manufacturer's instructions. Briefly, 0.5  $\mu$ g total RNA from each sample was mixed with diluted Spike Mix and T7 Promoter Primer Mix followed by incubation at 65°C for 10 minutes. cDNA Master Mix (5 $\times$  first-strand buffer, 0.1 M DTT, 10 mM dNTP mix, RNase-Out, and M-MLV reverse transcriptase enzyme) was prepared and added to the reaction mixture. Amplified and labeled cRNA was purified on RNase Mini Spin Columns (Qiagen, Hilden, Germany) according to the manufacturer's protocol. The labeled cRNA target was quantified using an ND-1000 spectrophotometer (NanoDrop Technologies, Wilmington, DE). After checking labeling efficiency, each 750-ng sample of cyanine 3-labeled and cyanine 5-labeled cRNA target was mixed, and cRNA fragmentation was performed by adding 10 $\times$  blocking agent, 25 $\times$  fragmentation buffer, and incubating at 60°C for 30 minutes. The fragmented cRNA was resuspended in 2 $\times$  hybridization buffer and directly pipetted onto an assembled Agilent Human GE 4x44K microarray. The arrays were hybridized at 65°C for 17 hours using an Agilent hybridization oven. The hybridized microarrays were washed according to the manufacturer's washing protocol (Agilent Technology).

### Data Acquisition and Analysis

The hybridized images were analyzed by an Agilent DNA microarray scanner, and data quantification was performed using the Agilent Feature Extraction software. The average fluorescence intensity for each spot was calculated, and local background was subtracted. All data normalization and selection of fold-changed genes were performed using GeneSpring GX 7.3 (Agilent Technology). Genes were filtered by removing the flagged-out genes in each experiment. Intensity-dependent normalization (Lowess) was performed, where the ratio was reduced to the residual of the Lowess fit of the intensity versus ratio curve. The means of the normalized ratios were calculated by dividing the average of normalized signal channel intensity by the average of normalized control channel intensity. Functional annotation of genes was performed according to criteria of the Gene Ontology Consortium (<http://www.geneontology.org/index.shtml>)

using GeneSpring GX 7.3. Gene classification was based on searches performed on BioCarta (<http://www.biocarta.com/>), Database for Annotation, Visualization, and Integrated Discovery (DAVID; <http://david.abcc.ncifcrf.gov/>), and MEDLINE databases (<http://www.ncbi.nlm.nih.gov/>). Bioinformatic gene network analyses were performed using IPA (<http://www.ingenuity.com>) to examine the biological functions of differentially regulated genes and proteins according to ontology-related interaction networks. IPA provides protein interaction networks based on the regularly updated “ingenuity pathways knowledgebase.” The network is optimized to include as many proteins from the input expression profile as possible and aims to produce highly connected networks.

### Real-Time PCR

The sequences of forward and reverse primers for FOXO3 (NM\_001455), HIF-1A (NM\_181054), and MEF2A (NM\_001171894) were as follows: FOXO3 (forward) 5'-ACA TGG GCT TGA GTG AGT CC-3' and (reverse) 5'-GCC TGA GAG AGA GTC CGA GA-3'; HIF1A (forward) 5'-TGC ATC TCC ATC TCC TAC CC-3' and (reverse) 5'-CCT TTT CCT GCT CTG TTT GG-3'; and MEF2A (forward) 5'-TCA GCT CTC TTG TTG CTG GA-3' and (reverse) 5'-AAA TCG GTT CGG ACT TGA TG-3'. The forward primer sequence for GAPDH (NM\_002046) was 5'-GGT CTC CTC TGA CTT CAA CA-3', and the reverse primer sequence was 5'-AGC CAA ATT CGT TGT CAT AC-3'. Total RNA (1 µg) was reverse transcribed to cDNA according to the manufacturer's instructions (M-MLV Reverse Transcriptase; Invitrogen, Carlsbad, CA). Reactions were carried out on an ABI Prism® 7900HT Sequence Detection System (PE Applied Biosystems, Foster City, CA), and relative transcript levels were determined using GAPDH as the endogenous control (SYBR Green method). Each reaction was performed in triplicate. Thermal cycling conditions were 95°C for 10 minutes followed by 45 cycles of 95°C for 10 s, 60°C for 15 s, and 72°C for 20 s. Data were analyzed using the Sequence Detection System software (SDS version 2.0, PE Applied Biosystems).

### Biochemical Analysis

Small interfering RNAs (siRNAs) were purchased from ST Pharm (Seoul, Korea). The nucleotide sequence for HIF-1A siRNAs was 5'-AAG TCT GCA ACA TGG AAG GTA-3' (NM\_181054.2), for FOXO3 siRNA was 5'-GTG GAG CTG GAC CCG GAG T-3' (NM\_201559.2), and that for MEF2A siRNA was 5'-AAG CCT ATG AAC TTA GTG TGC-3' (NM\_005587.2). Transfection of siRNAs into HepG2 cells was performed using Lipofectamine RNAiMAX reagent (Invitrogen, Carlsbad, CA) in accordance with the manufacturer's instructions. Cells were then treated with 10 µg/mL *H cordata* for 48 hours.

### Tumor Xenograft Experiment

For tumor xenograft experiments,  $1 \times 10^6$  HepG2 cells suspended in DMEM were injected subcutaneously into the hind limb of 5-week-old nude (nu/nu Balb/c) mice, which were then treated with PBS (6 mice) or 20 mg/kg *H cordata* EtOAc fraction (6 mice) once daily for 20 days. The mice were housed in a facility approved by the Association for Assessment and Accreditation of Laboratory Animal Care on a 12-hour light/12-hour dark cycle with food and water ad libitum. The mice were killed humanely 21 days postinjection. Tumors were fixed with 4% paraformaldehyde in PBS. The animal study was reviewed and approved by the Institutional Animal Care and Use Committee of the Korea Basic Science Institute.

### Immunohistochemistry

A 5-mm-thick section was cut across the dorsoventral diameter of the tumor and fixed in ice-cold 10% paraformalin overnight and embedded in paraffin. Serial sections (4-µm thick) were cut and processed for immunohistological staining. Paraffin sections on the microslides were deparaffinized in xylene and rehydrated in sequential ethanol baths. Antigen retrieval was achieved by incubation with 10 mM citrate buffer (pH 6.0) in a domestic microwave oven at 700 W for 30 minutes. The slides were quenched in hydrogen peroxide (3%) to block endogenous peroxidase activity and washed in TBS (0.05 M, pH 7.6). The slides were blocked with 3% BSA in PBS for 1 hour at room temperature and incubated overnight at 4°C with primary antibodies against the following: MEF2A (1:500; Dako), HIF-1A (1:500), and FOXO3 (1:500). The Labeled Streptavidin Biotin kit (Dako) based on the avidin-biotin peroxidase complex method was used for detection, and slides were counterstained with hematoxylin. Slides were dehydrated in sequential ethanol baths, rinsed with xylene, and mounted with Permount (ThermoFisher, Pittsburgh, PA).

### Image Acquisition and Protein Quantification

Samples were analyzed with a Zeiss AxioImagerZ1 microscopy system with a charge-coupled device camera and the TissueFAXS automated acquisition system (TissueGnostics, Vienna, Austria). The percentages of antibody-positive and stemness marker-positive tumors were determined and depicted as scattergrams. Images were digitalized, and protein expression was quantified. Statistical analysis was performed with the HistoQuest software (TissueGnostics).

### Statistical Analysis

For gene expression profiles obtained by microarray, data analysis was performed using GeneSpring GX version 7.3 (Agilent Technologies). Differentially expressed genes

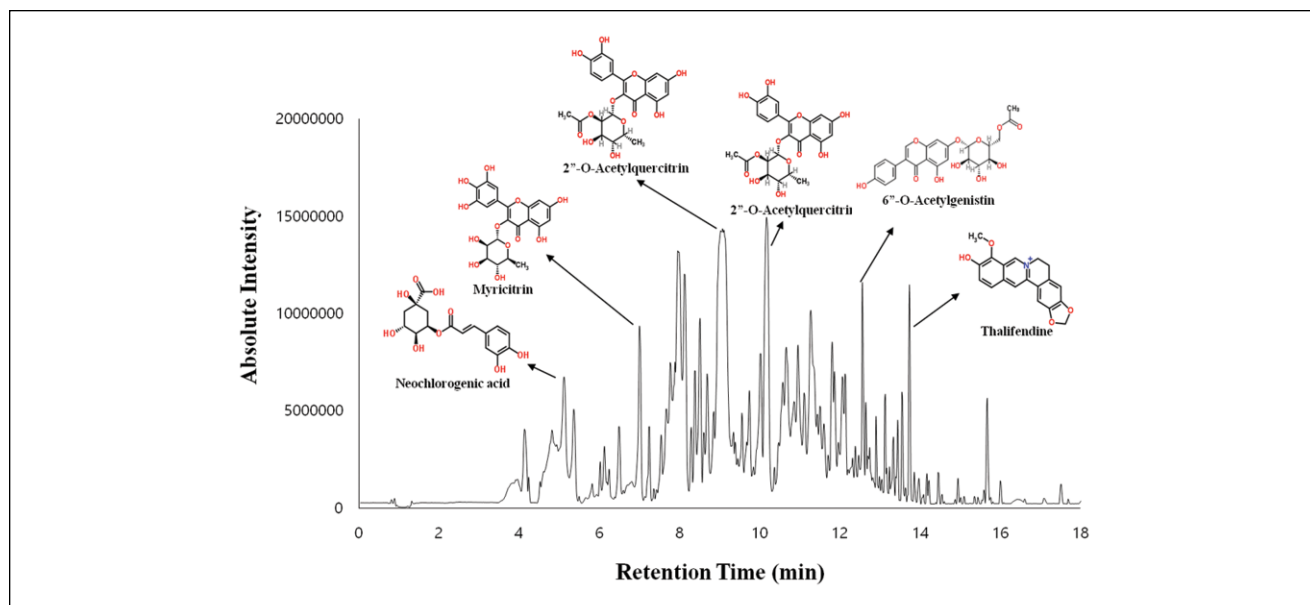


**Figure 1.** Quantification of *Houttuynia cordata* extract. Multiple reaction monitoring is the most common mode of using a triple quadrupole LC-MS for quantitative analysis; 100 mg of extract was mixed with 1 mL of methanol. Aliquots of 5  $\mu$ L of the processed samples were injected into the HPLC system. Data acquisition was performed with the MassHunter Software (version B.04.00).

were identified using the Student's *t*-test with a *P*-value cut-off of .05 and a fold-change threshold of 2.0. One-way analysis of variance (ANOVA) was used to determine significant differences between untreated control and treated samples. Reverse Transcription Polymerase Chain Reaction (RT-PCR) results were expressed as the mean  $\pm$  SD from at least 3 independent experiments. Data were analyzed using Student's *t*-test. *P* values <.05 were considered statistically significant.

## Results

### Quantification of *H cordata* Extract

LC-MS/MS analysis of *H cordata* extract revealed the presence of 5 compounds in the EtOAc, including neochlorogenic acid, myricitrin, 2''-O-acetylquercitrin, 6''-O-acetylgenistin, and thalifendine (Figure 1).

### Effect of *H cordata* Extract on Cell Death

The effect of *H cordata* extract on cell death was analyzed quantitatively using PI staining followed by flow cytometry (Figure 2A). Specifically, the relative proportion of viable and apoptotic cells can be measured on costaining with annexin V. Treatment of HepG2 cells with 1 and 10  $\mu$ g/mL *H cordata* extract led to the induction of late apoptosis. The proportion of apoptotic cells increased dramatically from 25.7% in control cells to 86.6% in cells treated with 10  $\mu$ g/mL of *H cordata* extract. However, no changes were observed after treatment with 1  $\mu$ g/mL of *H cordata* extract

(13.4%-15.7% early apoptotic cells and 24.4%-25.7% late apoptotic cells). Thus, HepG2 cells appeared to be sensitive to *H cordata* extract when used at 10  $\mu$ g/mL.

### Effect of *H cordata* Extract on Expression of Apoptotic Proteins

HepG2 liver carcinoma cells expressed Bax, Bcl-2, Bid, tBid, caspase-3, caspase-7, caspase-9, and PARP. Based on the observation that *H cordata* extract induces apoptosis in HepG2 cells, we examined the expression of apoptosis-related signaling proteins using western blot analysis (Figure 2B). *H cordata* extract treatment activated caspase-3- and caspase-7-mediated apoptosis. The expression of inactive caspase-3 (35 kDa) was decreased and that of active caspase-3 (17 kDa) increased with increasing concentrations of *H cordata* extract (Figure 2B). Other proapoptotic markers, such as Bax, increased slightly, whereas the antiapoptotic protein Bcl-2 showed decreased expression following *H cordata* extract treatment.

### Effect of *H cordata* Extract on Gene Expression Profiles

To identify the potential genes involved in the anticancer activity of *H cordata*, we performed a gene expression microarray in HepG2 hepatocellular cancer cells after treatment with *H cordata* extract. Among the 41 000 unique genes (using Agilent's Human GE 4x44K Microarray) tested, 18 732 genes were expressed in cells treated with 1

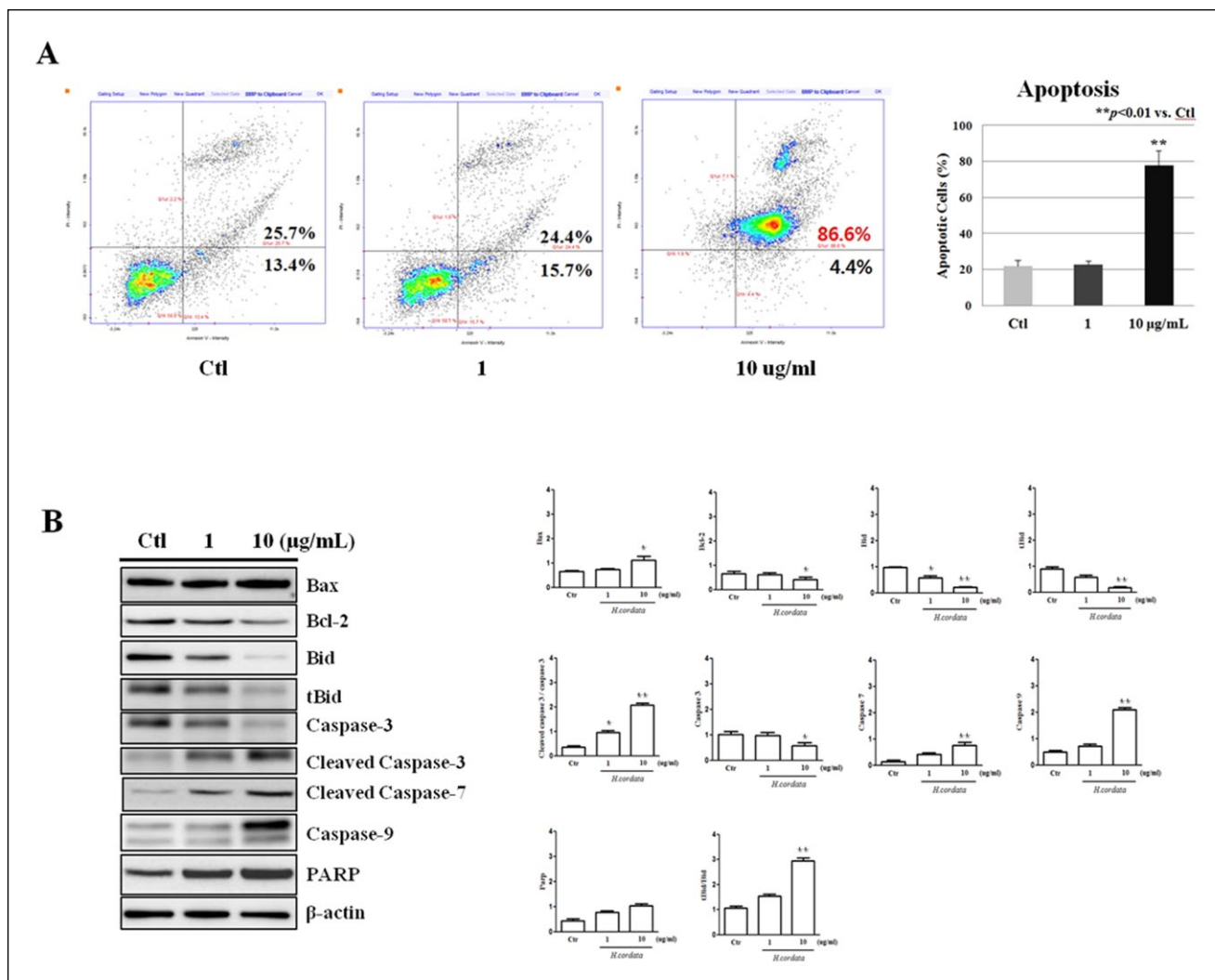


**Figure 2.** Analysis of apoptosis in HepG2 cells using flow cytometry and western blotting. (A) Effect of *Houttuynia cordata* extract on cell death. The proportion of apoptotic cells increased dramatically from 25.7% in control (Ctl) cells to 86.6% in cells treated with 10  $\mu\text{g/mL}$  of *H cordata* extract. However, no changes were observed after treatment with 1  $\mu\text{g/mL}$  of *H cordata* extract (13.4%-15.7% early apoptotic cells and 24.4%-25.7% late apoptotic cells). Cells were double stained with propidium iodide and annexin V. The lower-left quadrant indicates normal cells; the lower-right quadrant shows early apoptotic cells; and the upper-right quadrant shows the late apoptotic cells. Data are representative of 3 independent experiments. Bar graph showing results of *H cordata* extract-treated apoptotic cells. (B) Expression of apoptotic proteins in response to *H cordata* extract. Protein expression levels were determined by western blotting. The y-axis indicates the relative expression level obtained by western blotting.

or 10  $\mu\text{g/mL}$  of *H cordata* extract. Among these 18732 genes, 950 and 1910 genes were upregulated by treatment with both 1 and 10  $\mu\text{g/mL}$  *H cordata* extracts compared with the untreated control at 6 hours. Conversely, these treatments downregulated 117 and 693 genes, respectively. The genes that were upregulated or downregulated by more than 2-fold were significantly handled in data mining categories.

Biologically relevant features were constructed using the DAVID tools (<http://david.abcc.ncifcrf.gov/>). Gene lists corresponding to 2-fold up- and downregulation in the *H cordata* extract-induced liver cancer cells were uploaded to DAVID

for Gene Ontology analysis (Figure 3A left panel). Upregulated genes included those involved in the regulation of mRNA transcription, cell cycle, apoptosis, and chromosome segregation. Downregulated genes included those involved in chromosome organization, negative regulation of cell proliferation, and response to stress. To compare the results obtained on *H cordata* extract treatment with potential genes that are involved in apoptosis, we identified candidate genes using the GeneCards database (<http://www.genecards.org/>). The intersection obtained by hierarchical clustering is presented along with the gene lists in Figure 3A (right panel). The signal network of apoptotic genes in response to glucose is shown in Figure 3B.

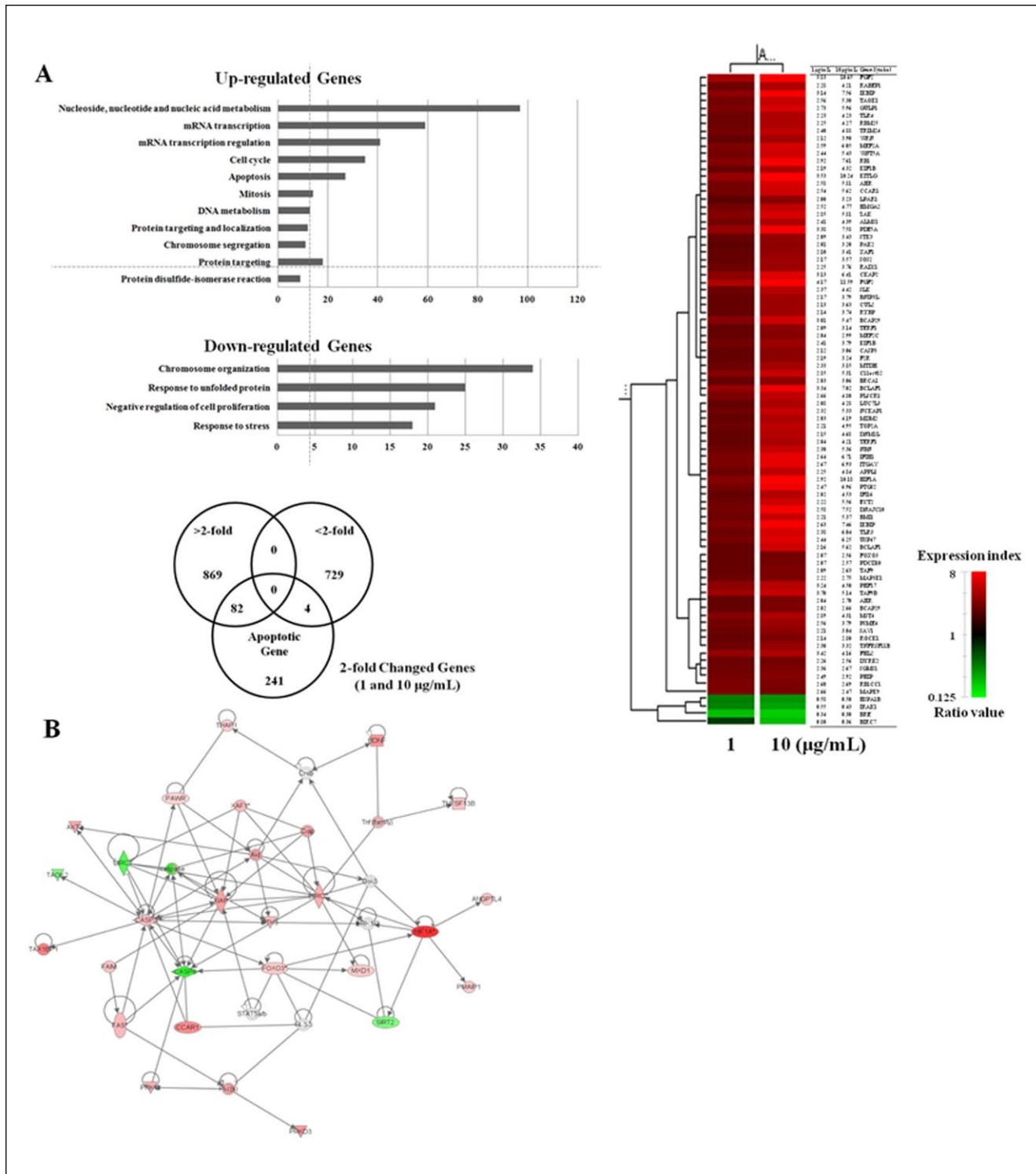


**Figure 3.** Gene ontology analysis and signal network of apoptotic genes. (A) Gene lists corresponding to 2-fold up- and downregulation in HepG2 cells treated with *Houttuynia cordata* extract for 6 hours (early time point). Greater than 2-fold upregulated and <2-fold downregulated genes and apoptotic genes are then individually intersected with Venn diagrams. A dendrogram of hierarchical clustering revealed the apoptosis genes induced by *H cordata* extract at 1 and 10 µg/mL compared with the control (ctl). The red and green colors represent >2-fold up- and downregulated genes, respectively. (B) Colored nodes as determined by IPA (Qiagen) are the genes in the apoptosis regulatory network in HepG2 cells (A).

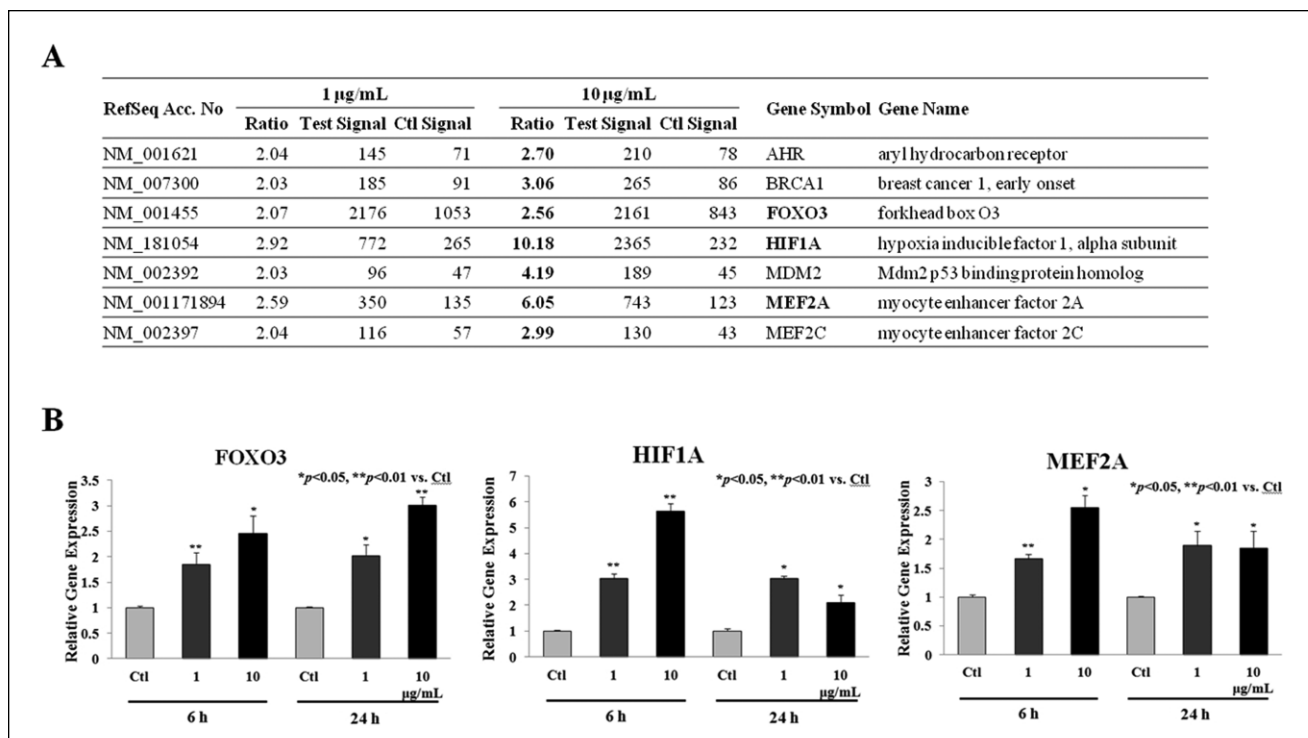


**Figure 4.** Gene expression of transcriptional regulators of apoptotic genes. Relative expression levels of Forkhead box (FOX)O3 (A), hypoxia-inducible factor (HIF)-1A (B), and MEF2A (C) genes were determined by RT-PCR. Each value represents mean  $\pm$  SD of triplicate experiments. \* $P < .05$ , \*\* $P < .01$  compared with control (ctl).

### Effect of *H cordata* Extract on Expression of Transcriptional Regulators

Upstream regulator analysis using IPA identified the upstream regulators (transcription regulators) of the apoptotic network (eg, AHR, BRCA1, FOXO3, HIF-1A, MDM2, MEF2A, and MEF2C) when comparing *H cordata* extract treatment to untreated cells (control; Figure 4A). Based on the microarray results, the expression levels of 3 upstream regulators (transcription regulators: FOXO3, HIF-1A, and MEF2A) were evaluated using RT-PCR. RT-PCR evaluation indicated that the expression levels of these upstream regulators were increased (about 2.5, 5.5, and 2.5-fold, respectively) in a time-dependent manner on treatment with 1 and 10  $\mu\text{g/mL}$  of *H cordata* extract, especially FOXO3 at 6 and 24 hours, when compared with controls (Figure 4B).

### *H cordata* Regulated the Expression and Intracellular Localization of FOXO3

To investigate whether *H cordata* affected the expression of FOXO3 and HIF-1A, we analyzed the levels of HIF-1A, FOXO3, and MEF2A in HepG2 cells under treatment with *H cordata*. Western blot assay revealed that *H cordata* significantly enhanced the expression of HIF-1A, FOXO3 (all nucleus and cytosol), and MEF2A in a time-dependent manner within 6 to 24 hours (Figure 5A). Akt can phosphorylate

FOXO transcription factors, which stimulates proteasomal degradation. Therefore, we investigated the levels of Akt phosphorylation (p-Akt) and also examined whether p-Akt affected FOXO3 activation. p-Akt was significantly decreased in HepG2 cells under *H cordata* treatment (Figure 5A).

### FOXO3 Affects the Expression of Bcl-2 Family of Proteins in HepG2 Cells Treated With *H cordata*

To assess the apoptotic process, we performed western blot analysis to evaluate the potential effect of FOXO3 on protein levels of the Bcl-2 family. Our results revealed that FOXO3 silencing increased Bcl-2 and Bcl-xL expression, whereas it decreased Bax, indicating that FOXO3 regulated the transcription levels of the Bcl-2 protein family (Figure 5B). These data suggested that the HIF-1A FOXO3 pathway is responsible for *H cordata*-induced disturbance of Bcl-2 family of proteins.

### HIF-1A Modulated *H cordata*-Induced FOXO3 Expression in HepG2 Cells

To investigate the effect of HIF-1A on *H cordata*-mediated expression of FOXO transcription factors, we inhibited HIF-1A activation by siRNA. Western blot results revealed that HIF-1A expression increased rapidly in HepG2 cells



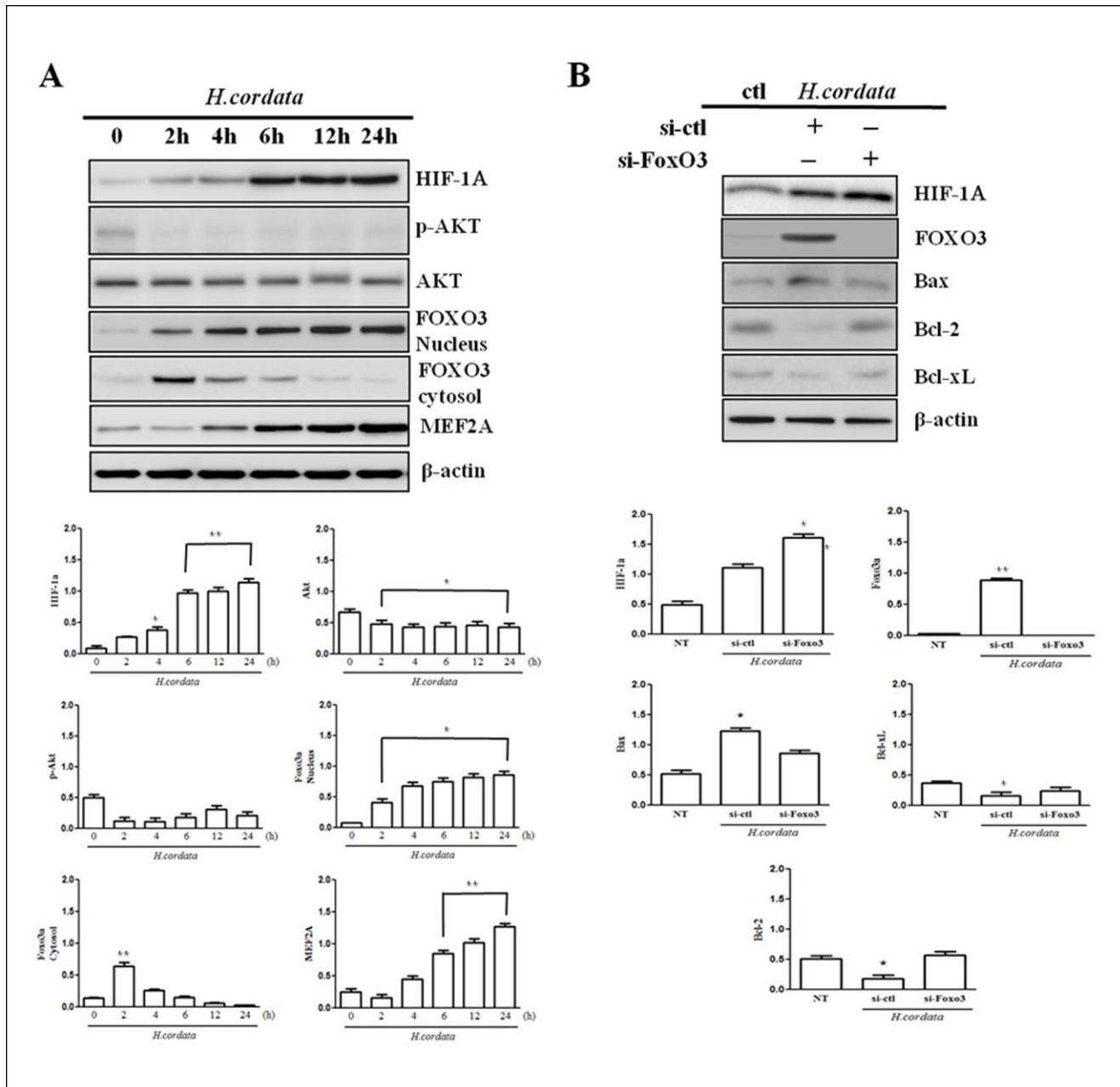


**Figure 5.** *Houttuynia cordata* promotes activation of hypoxia-inducible factor (HIF)-1A Forkhead box (FOX)O3 pathways by regulating Akt/PKB signaling. (A) *H cordata* increases HIF-1A expression, decreases Akt activity, and regulates the expression of FOXO3 in a time-dependent manner. Representative western blots of HIF-1A, p-Akt, Akt, and FOXO3 in HepG2 cells treated with *H cordata* extract. (B) FOXO3 affected the expression of Bcl-2 family of proteins in HepG2 cells. HepG2 cells were incubated with siRNA directed against FOXO3 (FOXO3 siRNA) followed by western blotting. Representative blots of HIF-1A, FOXO3, and Bcl-2 proteins, including Bcl-xl, Bcl-2, and Bax are shown. The y-axis indicates the relative expression level obtained by western blotting. Abbreviation: ctl, control.

under *H cordata* treatment, which was reduced after transient transfection with HIF-1A siRNA (Figure 6A). Western blot assay demonstrated that *H cordata* increased FOXO3 and p-FOXO3 protein levels, which were abolished on HIF-1A silencing (Figure 6A), indicating that HIF-1A increased FOXO3 transcription. Moreover, FOXO3

increased Bax expression, whereas decreasing Bcl-2 and Bcl-xL expressions were also reversed by HIF-1A silencing (Figure 6A). These data indicate that *H cordata*-induced FOXO3 expression in HepG2 cells was modulated at least in part by HIF-1A and that HIF-1A increases FOXO3 transcription during apoptosis.

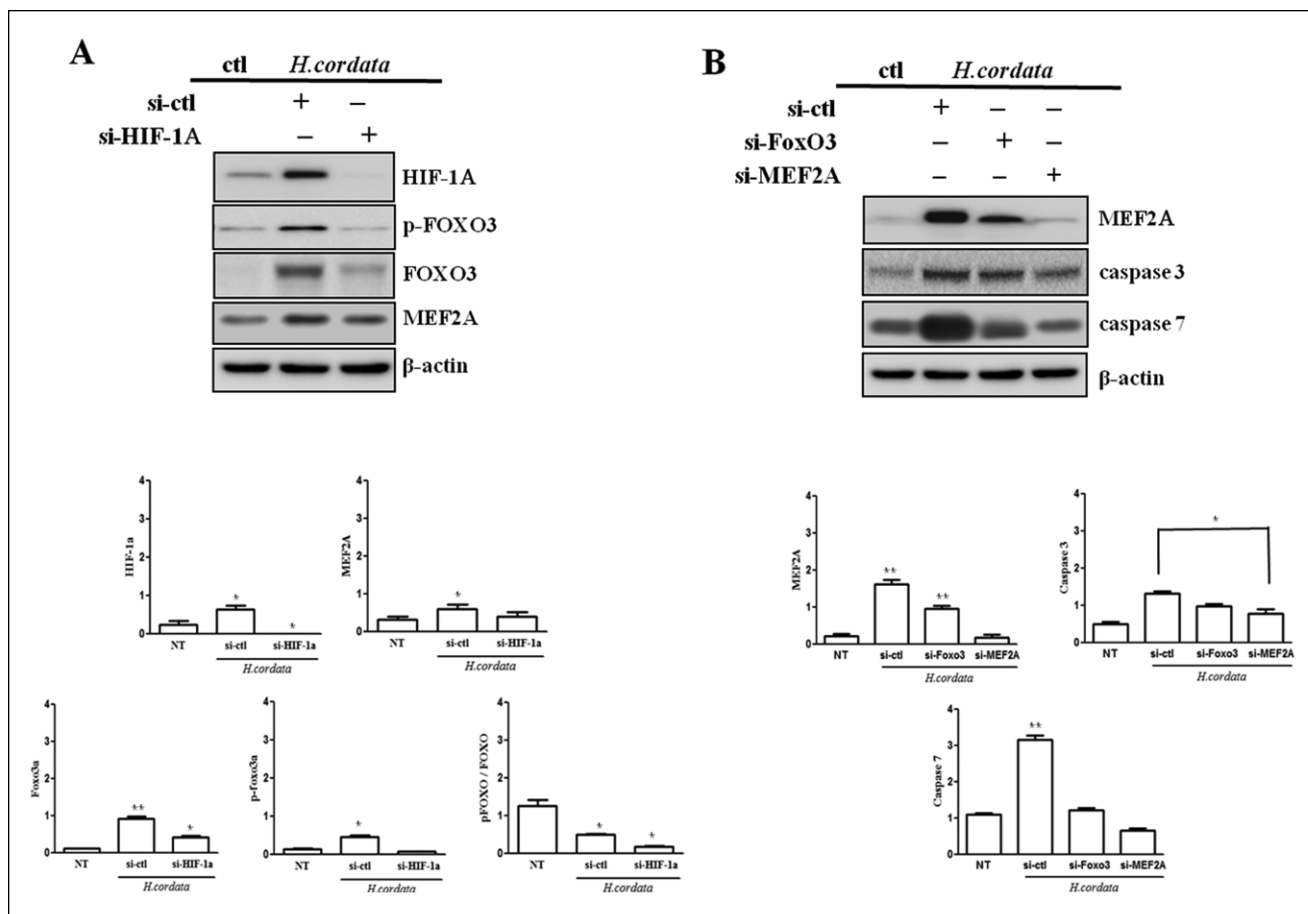


**Figure 6.** Hypoxia-inducible factor (HIF)-1A promotes the activation of MEF2A pathway directly and indirectly via Forkhead box (FOX)O3. (A) HIF-1A modulated FOXO3 activation and MEF2A expression induced by *Houttuynia cordata* extract in HepG2 cells. HepG2 cells were incubated with siRNA directed against HIF-1A (HIF-1A siRNA) for 6 hours. Western blot assay was performed to evaluate the expression of HIF-1A, FOXO3, p-FOXO3, and MEF2A. (B) FOXO3 regulates *H cordata*-induced MEF2A accumulation, caspase-3, and caspase-7 in HepG2 cells. HepG2 cells were incubated with siRNA directed against FOXO3 (FOXO3 siRNA) or control RNA (ctl siRNA) for 6 hours and assessed by western blotting. Representative blots of MEF2A, caspase-3, and caspase-7 proteins are shown. The y-axis indicates the relative expression level obtained by western blotting.

### *H cordata*-Mediated FOXO3 Expression Upregulates MEF2A and Activates Apoptosis-Associated Caspases

Upregulation of MEF2A was detectable at 6 hours after treatment with *H cordata* and was consistently observed after treatment with *H cordata* for 24 hours (Figure 6A). Inhibition of FOXO3 by siRNA transfection significantly reduced MEF2A expression in HepG2 cells under *H cordata*. These data indicate that FOXO3 contributes to *H cordata*-induced MEF2A expression. We analyzed the expression of MEF2A and apoptotic proteins in HepG2 cells transfected with FOXO3 siRNA. As shown in Figure 6B, FOXO3 silencing significantly reduced MEF2A, caspase-3, and caspase-7. MEF2A silencing also reduced caspase-3 and caspase-7 expression. These data indicate that FOXO3 upregulates MEF2A expression, resulting in apoptosis induced via caspase-3 and caspase-7 activation.

### Effect of *H cordata* EtOAc Fraction on Expression of MEF2A, HIF-1A, and FOXO3 in Human Hepatocellular Carcinoma Xenografts

We next assessed whether there was increased expression of MEF2A, HIF-1A, and FOXO3 in *in vivo* xenograft models. The expressions of MEF2A, HIF-1A, and FOXO3 were slightly increased by *H cordata* EtOAc fraction in HepG2 xenografts at 20 days compared with untreated controls (Figure 7).

## Discussion

This study examined the biological effects of *H cordata* on human liver HepG2 hepatocellular carcinoma cells. We performed a cytotoxicity test to calculate the 50% growth inhibitory ( $GI_{50}$ ) concentration of *H cordata* using an MTT assay to determine the challenging dose for microarray analysis. After 24 hours of incubation, the *H cordata* extract

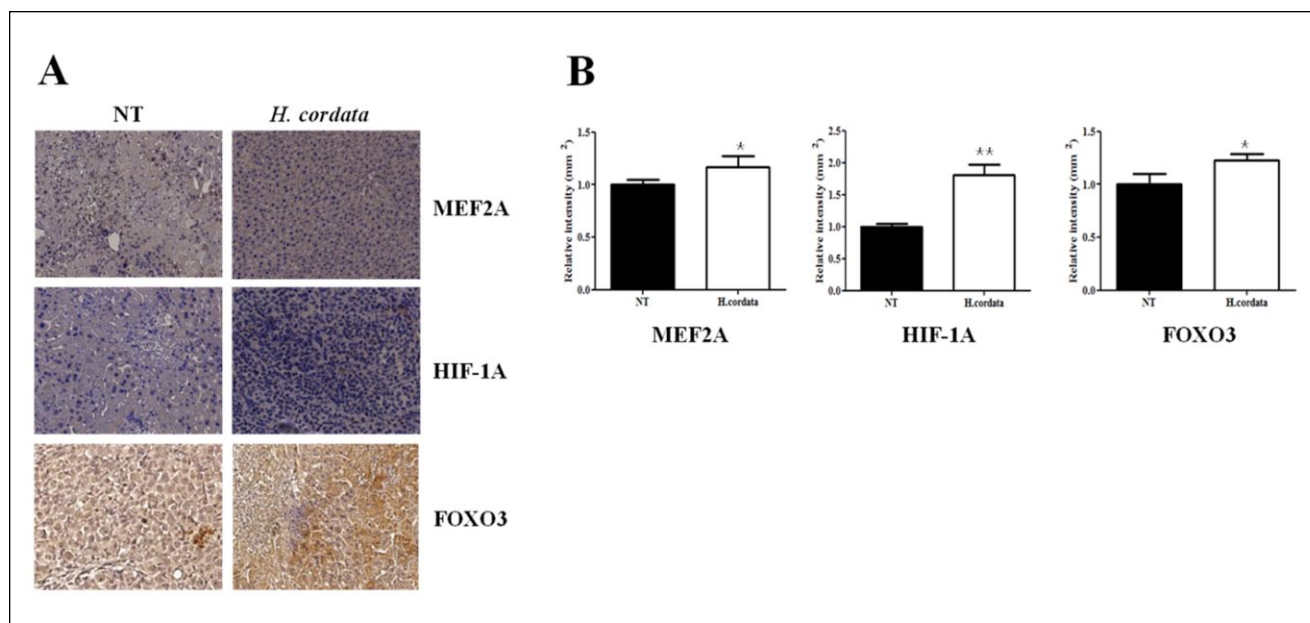


**Figure 7.** Effect of *Houttuynia cordata* ethyl acetate fraction on expression of MEF2A, hypoxia-inducible factor (HIF)-1A, and Forkhead box (FOX)O3 in human hepatocellular carcinoma xenografts. (A) Immunohistochemical staining for MEF2A, HIF-1A, and FOXO3. Nude mice were injected with HepG2 cells and then treated with PBS (6 mice) or 20 mg/kg *H cordata* (6 mice) once daily for 20 days. Tumor tissues were collected in 10% ice-cold paraformaldehyde and paraffin-embedded blocks were prepared for immunohistochemistry of MEF2A, HIF-1A, and FOXO3. (B) Quantification of MEF2A, HIF-1A, and FOXO3. Data are presented as the mean  $\pm$  SD of 3 independent experiments performed in triplicate. \* $P < .05$ , \*\* $P < .01$  versus untreated controls.

showed moderate activity with a  $GI_{50}$  of 10  $\mu\text{g}/\text{mL}$  (data not shown). We determined the effects of *H cordata* on the cell cycle and on cell death after incubation of HepG2 cells with the *H cordata* extract for 24 hours. *H cordata* extract at 10  $\mu\text{g}/\text{mL}$  induced a significant increase in HepG2 apoptosis (Figure 2A). Apoptosis of HepG2 cells by *H cordata* extract was also associated with downregulation of antiapoptotic Bcl-2 and upregulation of proapoptotic Bax protein expression. *H cordata* extract treatment induced proteolytic activation of caspase-3, caspase-7, and caspase-9 protein expression (Figure 2B). These results were inconsistent with those of a previous study demonstrating that *H cordata* extract induces proteolytic activation of caspase-3<sup>6</sup> in human lung cancer A549 cells. The apoptotic signaling pathway was also observed in HepG2 cells treated with *H cordata* extract in a microarray (Figure 3). Interestingly, many kinds of transcriptional regulators were induced after treatment with *H cordata* extract (Figure 4A). The expression levels of these transcriptional regulators—such as FOXO3 (red-colored node in Figure 4A), HIF-1A (red-colored node in Figure 4A), and MEF2A—in the *H cordata* extract-treated HepG2 cells were confirmed by RT-PCR and western blot in a dose- and time-dependent manner (Figure 4B, 5A). The expressions of MEF2A, HIF-1A, and FOXO3 were also slightly increased in xenografts (Figure 7). These findings suggest the possibility that HIF-1A, FOXO3, and MEF2A function are significant regulators in *H cordata*-mediated apoptosis of HepG2 cells. Parody

et al<sup>20</sup> reported that FOXO3, a member of the FOXO family, triggers the mitochondrial apoptotic pathway in the rat preneoplastic liver through modulation by interferon  $\alpha 2b$ . To our knowledge, this is the first demonstration of the role of HIF-1A and FOXO3 in *H cordata*-induced cancer cell apoptosis. Thus, the underlying mechanism of HIF-1A and FOXO3 pathways in *H cordata*-induced cancer cell apoptosis is still not fully understood. In this study, we revealed that FOXO3 upregulated Bax and downregulated Bcl-2 (Figure 5B) and that HIF-1A increased FOXO3 expression under *H cordata* treatment (Figure 6A). Furthermore, activation of the transcription factor FOXO3 causes MEF2A to induce the activation of caspase-3, caspase-7, and Bax, in addition to disturbing the expression of Bcl-2 family proteins, which are critical mediators of apoptosis in HepG2 cells (Figure 5B, 6B). In mammals, the ability of FOXO factors to mediate cell cycle arrest, DNA repair, and apoptosis makes them attractive as tumor suppressor candidates.<sup>17,19</sup> In this study, we investigated FOXO3 expression in HepG2 cells and identified a novel connection between FOXO3 and *H cordata*-induced apoptosis. siRNA-mediated HIF-1A inhibition also attenuated p-FOXO3 (Figure 6A). FOXO transcription factors can be phosphorylated by Akt, a serine/threonine-specific protein kinase. p-Akt attenuates FOXO3 translocation into the nucleus, its binding with 14-3-3 protein, and eventual proteasomal degradation. Our results revealed that *H cordata* attenuated p-Akt in a time-dependent manner (Figure 5A) and that *H cordata*

treatment resulted in a significant increase in the expression of HIF-1A and FOXO3 (Figures 5A and 5B), indicating that *H cordata* decreased the proteasomal degradation of FOXO3.

In a previous study, a pivotal role for the Reactive Oxygen Species-p38 Mitogen activated Protein kinase (ROS-p38 MAPK) axis was demonstrated in controlling the tumor-initiating capacity of glioma-initiating cells (GICs).<sup>21</sup> Meanwhile, the activation of the ROS-p38 axis has a significant inhibitory effect on tumor growth.<sup>22</sup> MEF2 is also activated via the p38-dependent pathway.<sup>23</sup> The p38-MEF2 pathway signals survival-promoting gene regulation, but when interrupted by excessive caspase activation, this pathway becomes proapoptotic.<sup>24</sup> Our results reveal that *H cordata*-mediated HIF-1A upregulated MEF2A directly (Figure 6A) and also indirectly via FOXO3 (Figure 6B). Based on these results and previous studies, we speculated that MEF2A functions as a significant regulator in *H cordata*-mediated apoptosis of HepG2 cells. Thus, activation of the ROS-p38 axis is responsible for MEF2A expression, suggesting that the ROS-p38-MEF2 pathway becomes proapoptotic on excessive caspase-3 and caspase-7 activation. Taken together, the multipathway proapoptotic function and the unique activation of HIF-1A-FOXO3 and MEF2A pathways suggest that *H cordata* may be a promising natural product extract for potential use in liver cancer. We found that *H cordata* induces apoptosis through the activation of transcription regulators, such as HIF-1A, FOXO3, and MEF2A. It will also be important to identify the precise cellular targets of *H cordata*, which may help further elucidate the mechanisms of its antitumor functions and contribute to the development of more effective anticancer drugs.

## Conclusions

Our results demonstrate that *H cordata*-mediated HIF-1A upregulates MEF2A directly and also indirectly via FOXO3 in HepG2 cells. Thus, we have demonstrated that *H cordata* shows anticancer activity in liver cancer cells by inducing apoptosis through activation of transcription regulators, such as HIF-1A, FOXO3, and MEF2A. These findings not only suggest that an EtOAc fraction derived from *H cordata* is a promising natural extract for potential use in liver cancer therapy, but also demonstrate that exploring compounds capable of inducing apoptosis and activity of upstream transcription regulators is a promising strategy for drug discovery against liver cancer.

## Declaration of Conflicting Interests

The author(s) declared no potential conflicts of interest with respect to the research, authorship, and/or publication of this article.

## Funding

The author(s) disclosed receipt of the following financial support for the research, authorship, and/or publication of this article: this work was supported by a grant from the Wonkwang University in 2014.

## References

- Chen X, Wang Z, Yang Z, et al. *Houttuynia cordata* blocks HSV infection through inhibition of NF-kappaB activation. *Antiviral Res.* 2011;92:341-345.
- Miyata M, Koyama T, Yazawa K. Water extract of *Houttuynia cordata* Thunb. leaves exerts anti-obesity effects by inhibiting fatty acid and glycerol absorption. *J Nutr Sci Vitaminol (Tokyo)*. 2010;56:150-156.
- Tang YJ, Yang JS, Lin CF, et al. *Houttuynia cordata* Thunb extract induces apoptosis through mitochondrial-dependent pathway in HT-29 human colon adenocarcinoma cells. *Oncol Rep.* 2009;22:1051-1056.
- Lai KC, Chiu YJ, Tang YJ, et al. *Houttuynia cordata* Thunb extract inhibits cell growth and induces apoptosis in human primary colorectal cancer cells. *Anticancer Res.* 2010;30:3549-3556.
- Banjerdpongchai R, Kongtawelert P. Ethanol extract of fermented Thunb induces human leukemic HL-60 and Molt-4 cell apoptosis via oxidative stress and a mitochondrial pathway. *Asian Pac J Cancer Prev.* 2011;12:2871-2874.
- Chen YF, Yang JS, Chang WS, Tsai SC, Peng SF, Zhou YR. *Houttuynia cordata* Thunb extract modulates G0/G1 arrest and Fas/CD95-mediated death receptor apoptotic cell death in human lung cancer A549 cells. *J Biomed Sci.* 2013;20:18.
- de Araujo Junior RF, de Souza TP, Pires JG, et al. A dry extract of *Phyllanthus niruri* protects normal cells and induces apoptosis in human liver carcinoma cells. *Exp Biol Med (Maywood)*. 2012;237:1281-1288.
- Semenza GL, Rue EA, Iyer NV, Pang MG, Kearns WG. Assignment of the hypoxia-inducible factor 1alpha gene to a region of conserved synteny on mouse chromosome 12 and human chromosome 14q. *Genomics.* 1996;34:437-439.
- Hogenesch JB, Chan WK, Jackiw VH, et al. Characterization of a subset of the basic-helix-loop-helix-PAS superfamily that interacts with components of the dioxin signaling pathway. *J Biol Chem.* 1997;272:8581-8593.
- Chiavarina B, Whitaker-Menezes D, Migneco G, et al. HIF1-alpha functions as a tumor promoter in cancer associated fibroblasts, and as a tumor suppressor in breast cancer cells: autophagy drives compartment-specific oncogenesis. *Cell Cycle.* 2010;9:3534-3551.
- Ranasinghe WK, Sengupta S, Williams S, et al. The effects of nonspecific HIF1alpha inhibitors on development of castrate resistance and metastases in prostate cancer. *Cancer Med.* 2014;3:245-251.
- Ranasinghe WK, Xiao L, Kovac S, et al. The role of hypoxia-inducible factor 1alpha in determining the properties of castrate-resistant prostate cancers. *PLoS One.* 2013;8:e54251.
- Bruick RK. Expression of the gene encoding the proapoptotic Nip3 protein is induced by hypoxia. *Proc Natl Acad Sci U S A.* 2000;97:9082-9087.

14. Sowter HM, Ratcliffe PJ, Watson P, Greenberg AH, Harris AL. HIF-1-dependent regulation of hypoxic induction of the cell death factors BNIP3 and NIX in human tumors. *Cancer Res.* 2001;61:6669-6673.
15. Accili D, Arden KC. FoxOs at the crossroads of cellular metabolism, differentiation, and transformation. *Cell.* 2004;117:421-426.
16. van der Horst A, Burgering BM. Stressing the role of FoxO proteins in lifespan and disease. *Nat Rev Mol Cell Biol.* 2007;8:440-450.
17. Skurk C, Maatz H, Kim HS, et al. The Akt-regulated forkhead transcription factor FOXO3a controls endothelial cell viability through modulation of the caspase-8 inhibitor FLIP. *J Biol Chem.* 2004;279:1513-1525.
18. Arden KC. FoxOs in tumor suppression and stem cell maintenance. *Cell.* 2007;128:235-237.
19. Zou Y, Tsai WB, Cheng CJ, et al. Forkhead box transcription factor FOXO3a suppresses estrogen-dependent breast cancer cell proliferation and tumorigenesis. *Breast Cancer Res.* 2008;10:R21.
20. Parody JP, Ceballos MP, Quiroga AD, et al. FoxO3a modulation and promotion of apoptosis by interferon-alpha2b in rat preneoplastic liver. *Liver Int.* 2014;34:1566-1577.
21. Sunayama J, Sato A, Matsuda K, et al. FoxO3a functions as a key integrator of cellular signals that control glioblastoma stem-like cell differentiation and tumorigenicity. *Stem Cells.* 2011;29:1327-1337.
22. Gentles AJ, Gallahan D. Systems biology: confronting the complexity of cancer. *Cancer Res.* 2011;71:5961-5964.
23. Suzuki E, Satonaka H, Nishimatsu H, et al. Myocyte enhancer factor 2 mediates vascular inflammation via the p38-dependent pathway. *Circ Res.* 2004;95:42-49.
24. Okamoto S, Li Z, Ju C, et al. Dominant-interfering forms of MEF2 generated by caspase cleavage contribute to NMDA-induced neuronal apoptosis. *Proc Natl Acad Sci USA.* 2002;99:3974-3979.